Britholite (–Y) and its alteration: Reiarsdal, Vest-Agder, south Norway. Contributions to the mineralogy of Norway, No. 64

WILLIAM L. GRIFFIN, BORGHILD NILSSEN & BRENDA B. JENSEN

Britholite (-Y) occurs as large crystals (5-20 cm) in a zoned granite pegmatite at Reiarsdal, Vest-Agder. Textures suggest that britholite and primary inclusions of a Mn-oxide phase reacted with fluids along fractures, to produce (1) fluorapatite + calcite + thalenite (s. l.) and (2) tombarthite. Microprobe analyses show that thalenite and tombarthite have essentially inherited the HREE-enriched REE pattern of the britholite. Thalenite appears to have equilibrated with britholite, but the heterogeneity of the tombarthite implies extensive disequilibrium and mobility of most elements during the late hydrothermal alteration of the britholite.

W. L. Griffin, B. Nilssen & B. B. Jensen, Mineralogisk-geologisk museum, Sars gt. 1, Oslo 5, Norway.

This note describes the first recorded occurrence of britholite (-Y) in the granite pegmatites of southern Norway. Primary and secondary inclusions in the britholite (-Y) are an Mn-oxide, apatite, calcite, thalenite, and tombarthite. This is the second recorded occurrence of tombarthite; petrographic and chemical features offer evidence for the hydrothermal origin of the tombarthite. The material described here was first brought to the authors' attention by A. Corneliussen of Evje, and more material was later collected by us, assisted by A. Corneliussen, Chr. Dale, T. Garmo, and J. Brommeland.

Locality

The locality is the lower of two small pegmatites occurring in an amphibolite on a knob above the farm Reiarsdal in Vennesla kommune, southwest of the Iveland-Evje district and outside the main Iveland-Evje amphibolite body. Both pegmatites crosscut the foliation of the surrounding amphibolite, and both were earlier quarried for quartz and feldspar. The lower quarry is approximately 6×15 m in area, and worked to a depth of about 4 m. A quartz core apparently made up 1/3 to 1/2 of the total volume. The outer zone consists of coarsely intergrown K-feldspar, plagioclase, and biotite. The minor minerals, including yttrotitanite, orthite, zircon (malakon), uraninite, and britho-

lite, are concentrated in a zone 1.5–2 m from the contact, just outside the quartz core. Britholite is the most abundant phase, other than quartz and feldspar, in this zone. It occurs as crystals 5–20 cm in cross section, some of which are intergrown with orthite.

Physical properties and petrography

Britholite is light tan to chocolate brown. and the freshest material has a greasy to adamantine luster on the conchoidal fracture surfaces. The hardness is between 5 and 6. The specific gravity was measured as 4.05 on a large fragment by Berman balance and as 4.014 on a small sliver in a pychnometer. The britholite contains microscopic inclusions of several phases (see below) but the effect of these on the density probably cancel one another, so that the measured value should be approximately correct for the britholite itself. An IR spectrum showed a large broad peak typical of metamict silicates, but no recognizable peaks for H_2O or OH^-.

The untreated material is X-ray amorphous. When heated to 1000°C for 20 hours, it yields a powder pattern typical of an apatite structure (Table 1). The cell parameters are $a_0 = 9.39$ Å, $c = 6.81$ Å, similar to those of 'abukumalites' from the USSR and Japan (Kupriyanova & Sidorenko 1963, Nagashima & Kato 1966). We are uncertain of the chemical content of this cell;

Table 1.

X-ray data for britholite(-Y).

Heated at 1000°C for 20 hours.

D(Å)	hkl	I (vis.est.)
4.07	200	m
3.88	111	m
3.41	002	m
3.22		w
3.15	102	m
308	201	m
2.80	211	st
2.76	112	m+
2.72	300	m+
2.62		w
2.66		w
2.37		w+
2.25	310	w+
2.04	113	w+
2.03	400	w+
1.93	222	st
1.88	312	m
1.86	320	w
1.82	213	m
1.77	410	m
1.74	402	m

a = 9.39; c = 6.81
V = 519.32; m = 709.52
$D_{calc.}$ = 4.54

our analyses are on unheated material, and Ito (1968) has demonstrated that appreciable changes in the ratio of divalent to trivalent cations can occur in this structure during recrystallization by heating.

In thin section the britholite is light brown; the intensity of color varies irregularly within each grain. It is isotropic, locally weakly anisotropic. The britholite locally contains abundant fine-grained inclusions, many of which are arranged in elongate trains defining a rough planar structure. These inclusions have been identified by optical characteristics and microprobe analysis (Table 2); their size made their isolation for X-ray difficult.

The most abundant inclusions are fluorapatite; the grains are very small (5–50 μm) and commonly arranged in a perthite-like texture. More obvious, because of their higher relief, are the thalenite inclusions. These are elongate, branching aggregates of grains up to 200 μm long; they have a large 2V, are optically positive, with low birefringence, and are commonly polysynthetically twinned. These inclusions are often associated with minor calcite. An opaque phase occurs in elongate grains similar in size and shape to those of thalenite, but sometimes larger (up to 300 μm). Microprobe analysis shows it to be manganese oxide or hydroxide, with minor amounts of Si, Ca and Y (Table 2). It takes an extremely poor polish, so that no satisfactory analyses could be obtained; hence identification of this phase is uncertain. It may be a ramsdellite/birnessite (MnO_2), or even braunite. This phase is commonly surrounded and corroded by tombarthite, often intergrown with calcite.

All of these inclusions are observed isolated from one another within the britholite. They are typically associated with thin, closely spaced fractures, along which calcite is also common. The same fractures have clearly guided the formation of tombarthite, which occurs as black stripes up to 2 mm wide in the britholite. Tombarthite begins to form as thin darker brown selvedges on the fractures and spreads along an irregular front into the britholite. As a result, zones of tombarthite typically include thalenite, apatite, and opaques. Near the fractures, and especially near the abundant opaque inclusions, the tombarthite is a dark reddish brown in thin section, while it pales to a light chocolate brown closest to fresh britholite. The mineral shows a patchy mosaic texture with very low birefringence.

The textural observations suggest that the manganese oxide phase may be a primary inclusion in the britholite. The apatite, thalenite, and calcite are apparently secondary phases, formed by alteration (accompanied by exsolution?) along fractures. Tombarthite has clearly formed last, at the expense of both britholite and the opaque phase.

Analyses

Electron microprobe analyses were carried out using a manual ARL-EMX probe at Sentralinstitutt for industriell forskning, Oslo. Methods were those described by Åmli & Griffin (1975), and the errors are of a magnitude similar to those reported there. There is a severe interference of

Table 2.   Analyses of britholite and associated minerals.

	Britholite	Thalenite	Tombarthite (light)	Tombarthite (dark)	Type Tombarthite	Apathite	Opaque
SiO_2	22.0	30.0	14.8	20.5	12.6 – 15.9	1.6	2.8
P_2O_5	3.5	0.2	2.1	4.1	–	41.4	0.0
FeO	0.6	0.1	2.2	2.3	0.78– 5.52	0.2	0.25
MnO	0.9	0.05	4.9	10.0	3.68– 1.02	0.3	76.2
MgO	0.0	0.0	0.2	0.2	0.33– 0.26	0.0	1.1
CaO	15.3	0.07	4.7	4.4	3.56– 4.88	53.8	2.8
Y_2O_3	33.2	38.6	33.0	34.7	29.96–28.00	1.8	3.8
Lu_2O_3	2.6	6.7	2.5	0.79	0.93– 0.79	0.0	n.a.
Yb_2O_3	8.9	20.4	9.4	3.3	6.05– 5.79	0.05	"
Tm_2O_3	1.1	1.9	0.99	0.21	0.76– 0.64	0.0	"
Er_2O_3	2.8	3.2	2.4	0.7	4.24– 3.91	0.0	"
Ho_2O_3	1.0	0.44	0.9*	2.3*	1.08– 0.90	0.0	"
Dy_2O_3	1.3	0.66	1.2	0.36	4.19– 3.85	0.0	"
Tb_2O_3	0.02	0.01	0.00	0.00	0.47	0.0	"
Gd_2O_3	0.36	0.03	0.09	0.01	1.45– 1.53	0.0	"
Eu_2O_3	0.05	0.07	0.01	0.04	0.05	0.0	"
Sm_2O_3	0.09	0.05	0.12	0.07	0.58– 0.57	0.0	"
Nd_2O_3	0.36	0.00	0.40	0.55	0.52– 0.48	0.0	"
Pr_2O_3	0.05	0.00	0.14	0.12	0.08	0.0	"
Ce_2O_3	0.54	0.00	0.52	0.13	0.42	0.0	"
Ca_2O_3	0.11	0.00	0.08	0.15	0.06	0.0	"
UO_2	2.0	0.63	1.0	1.83	1.31– 0.57	0.35	"
ThO_2	1.9	0.0	6.1	1.3	3.08– 0.85	0.0	0.0
H_2O	0.45**	–	19.2	14.9	21.19–22.71		"
F	1.8	0.0	0.0	0.0		3.2	"
Σ	100.93	103.15	106.95	102.96		102.80	86.95
$O \equiv F$	0.76		7.6	7.9		1.46	
Σ	100.17		99.35	95.06		101.34	

* Strongly interfered by Mn, empirically corrected

** Remfield tube det.

Mn on $HoL\alpha$ in tombarthite. This has been empirically corrected for, but the Ho content of the dark variety (Table 2) is still ten times that expected from the Er and Dy contents. This anomaly could be real, but its cause is not clear. The Tb content of the britholite is much lower than would be expected given the Dy and Gd contents, but the precision is low because of very high background. The same applies to the tombarthites; if Tb_2O_3 is taken as equal to the detection limit (100 ppm), the Tb would appear in the REE plot (Fig. 1) at about the level expected from the Dy and Gd contents. Al, Cl, and Ti were all sought but not found (<0.1%). Minor Pb was detected in the britholite by XRF.

The britholite, thalenite, and apatite are quite homogeneous from point to point, and the analyses in Table 2 are averages of several analysis points within a single britholite crystal. The tombarthite is, in contrast, extremely heterogeneous, especially with regard to Fe, Mn, and Si. The analyses presented each represent averages of areas of about 300–500 μm^2. These areas were scanned during analysis, both to reduce destruction of the mineral by the beam and to obtain more representative analyses. The heterogeneity of the material has, however, reduced the quality of the analyses somewhat.

Britholite: The analysis (Table 2) shows this to be a calcium-yttrium silicate with minor phosphorous, which fits an idealized apatite formula $Ca_2Y_2Si_3O_{12}$ (OH,F) (Table 3). Kupriyanova & Sidorenko (1963) define britholite as an apatite structure with CaO 6–18%, SiO_2 13–28%, $(P_2O_5 + B_2O_3)$ 1.5–6.5%, $ThO_2 < 10\%$,
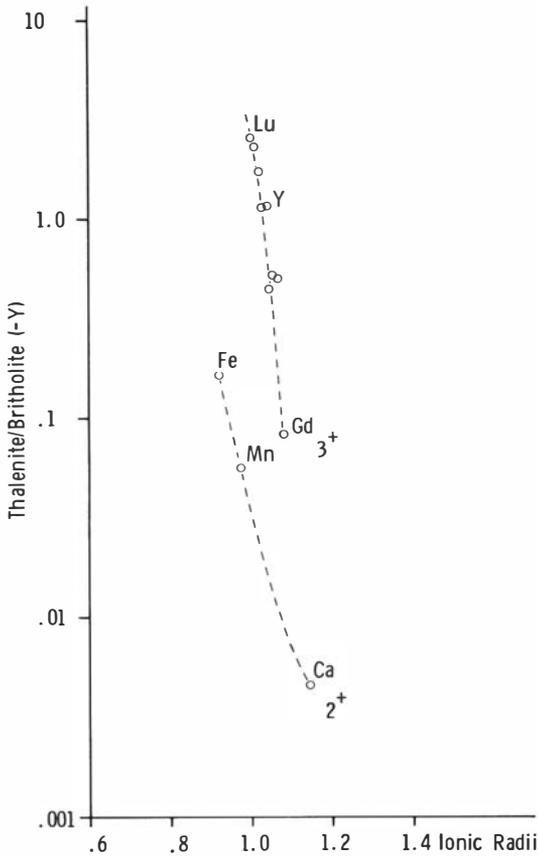
Fig. 1. Partition coefficients thalenite/britholite (-Y) as a function of ionic radii (ionic radii of Shannon & Prewitt (1969)).

Al_2O_3 < 5%, and the ratio P/B>>1. Boron cannot be analyzed by microprobe. However, the Reiarsdal mineral has 3.5% P_2O_5, and the analytical sum is satisfactory, so the B_2O_3 content is almost certainly less than 2%. The mineral thus meets the criteria for britholite.

The REE data (Fig. 1) show a strong enrichment in Y and the heavy REE; hence this is the variety britholite (-Y), formerly known as abukumalite. Nagashima et al. (1971) give analyses of 'abukumalite' from two Japanese localities, Fusamata and Suishoyama (type locality). The Fusamata material is generally similar to ours for major elements, especially the high F/OH and low P_2O_5 content, while both Japanese examples have relatively high (1%) Al_2O_3 contents. The only REE data on abukumalite available for comparison with the present analyses are a single analysis by Pletneva et al.

(1960). This analysis shows much less enrichment in Y and HREE than our material, but the poor quality of the analysis does not encourage detailed comparison.

The only other known occurrence of britholite in Norway is in the Permian nepheline-syenite dikes of the Tvedalen area near Larvik (G. Raade, Int. Rept. 35, Geologisk museum, 1971). This material has not been quantitatively analyzed, but optical spectrography shows it to be a britholite, while the cell parameters of the heated material (a_0 = 9.42 Å, c_0 = 6.92 Å) indicate that it probably is britholite (-Y) or aluminium britholite.

Thalenite: The analysis (Table 2) shows a nearly pure Y, REE silicate. The analytical sum is high, but the analysis calculates well to a (Y, $REE)_2Si_2O_7$ formula (Table 3). Recent studies (Kornev et al. 1972) indicate that the true formula of thalenite is $(Y,REE)_3Si_3O_{10}OH$. The present analysis may be calculated on this basis as well (Table 3), but this requires the presence of 1.53 wt% H_2O, whereas the high analytical sum suggests that little or no (OH) is present. It is therefore probable that the Reiarsdal mineral is not a true thalenite but a related, as yet unnamed, mineral that gives the X-ray pattern of $\beta-Y_2Si_2O_7$ (thortveitite-type structure; Warshaw & Roy 1964). This mineral occurs in a non-metamict state, together with fresh thalenite, at Åskagen, Sweden (a classic thalenite locality), and has also been found at Høgetveit, Evje (H. Neumann & B. Nilssen, pers. comm.) The inclusions in the Reiarsdal britholite are too small for X-ray diffraction studies; we will therefore use the name 'thalenite' (sensu lato) for this material until further information is available.

The REE pattern (Fig. 1) shows extreme enrichment in the heavy REE, while the light REE are below detection level (~100 ppm). There is a marked positive Eu anomaly, which is impossible to explain on the basis of crystal chemistry. However, the amounts of Sm, Eu, and Gd involved are small (300–700 ppm oxides), so that the anomaly may be due to analytical errors (Åmli & Griffin 1975), though this seems unlikely.

Nagashima & Kato (1966) describe thalenite that occurs in fist-sized crystals together with britholite (-Y) in the type locality of the latter at Suishoyama, Japan. This thalenite, which contains less REE than the present material, also has a much flatter REE pattern (Yb/Dy = 2.7, *vs*.

Table 3.   Structural formulae.

Basis	Brith.(-Y) Cat. = 5	Apatite Cat. = 5	Thalenite O = 7	O = 10.5	Tombarthite light Cat. = 4	Tombarthite dark Cat. = 4
Si	2.6068	0.1354	1.981	2.972	1.6434	2.2209
P	0.3509	2.9639	0.011	0.016	0.1973	0.3758
Fe	0.0594	0.0141	0.005	0.008	0.2042	0.2083
Mn	0.0903	0.0213	0.003	0.004	0.4607	0.9173
Ca	1.9415	4.8751	0.005	0.007	0.5589	0.5105
Y	2.0923	0.0923	1.325	1.988	1.9490	1.9995
Lu	0.0930	–	0.130	0.196	0.0835	0.0258
Yb	0.3214	0.0017	0.401	0.602	0.3182	0.1089
Tm	0.0405	–	0.038	0.057	0.3414	0.0070
Er	0.1042	–	0.065	0.097	0.0837	0.0238
Ho	0.0347	–	0.009	0.013	0.0317	0.0688
Dy	0.0496	–	0.014	0.021	0.0430	0.0126
Tb	0.0008	–	–	–	–	–
Gd	0.0142	–	0.001	0.001	0.0033	–
Eu	0.0020	–	0.001	0.002	0.0004	0.0015
Sm	0.0037	–	0.001	0.002	0.0046	0.0026
Nd	0.0152	–	–	–	0.0159	0.0213
Pr	0.0021	–	–	–	0.0057	0.0048
Ce	0.0234	–	–	–	0.0212	0.0051
La	0.0048	–	–	–	0.0033	0.0060
U	0.0527	0.0066	0.009	0.013	0.0247	0.0441
Th	0.0512	–	–	–	0.1541	0.0320
OH	0.3554	–	–	1.0	14.24	10.80
F	0.6742	0.8828	–	–	–	–

Britholite(-Y): $(Y,RE,Ca,U,Th,Mn,Fe)_{5.00}(Si,P)_{2.96}O_{12.26}F_{0.67}$

Apatite: $(Ca,Y,Yb,Fe,Mn,U)_{5.00}(P,Si)_{3.10}O_{12}F_{0.88}$

Thalenite: $(Y,RE,Fe,Mn,Ca,U)_{2.980}(Si,P)_{1.992}O_7$

or $(Y,RE,Fe,Mn,Ca,U)_{3.011}(Si,P)_{2.988}O_{10}OH$

Light tombarthite: $(Y,RE,Fe,Mn,Ca,U,Th)_{4.0}Si_{1.64}P_{0.20}(H_4)_{2.16}O_{10.4}OH_{5.6}$

Dark tombarthite: $(Y,RE,Fe,Mn,Ca,U,Th)_{4.0}Si_{2.22}P_{0.38}(H_4)_{1.40}O_{10.8}OH_{5.7}$

31 for the present material). Nagashima & Kato point out that most other thalenites for which REE data exist show an enrichment in Dy and the adjacent REE, where the ionic radii are closest to that of Y.

At Reiarsdal, the textural evidence suggests that the thalenite has formed from a britholite 'reservoir'. If this is the case, a plot of the partition coefficients (thalenite/britholite) versus ionic radius should give smooth curves with maxima indicating the optimum size of the large cation (Ca, Y, REE) site (Jensen 1973). Fig. 2 shows that such curves are in fact obtained. There is a steady increase in the partition coeffi-

cients with decreasing ionic radius and the curves for trivalent and divalent ions are sub-parallel. This supports the suggested genetic interpretation; it also implies that the optimum size of the (Y, REE) position in the thalenite is smaller than Y. The fact that the site is small also supports our tentative conclusion that this 'thalenite' is the β modification, isostructural with thortveitite ($Sc_2Si_2O_7$).

Tombarthite: The H_2O contents have been calculated from the structural formulae; the resulting analytical sums are comparable to those of the original wet-chemical analyses (Neumann
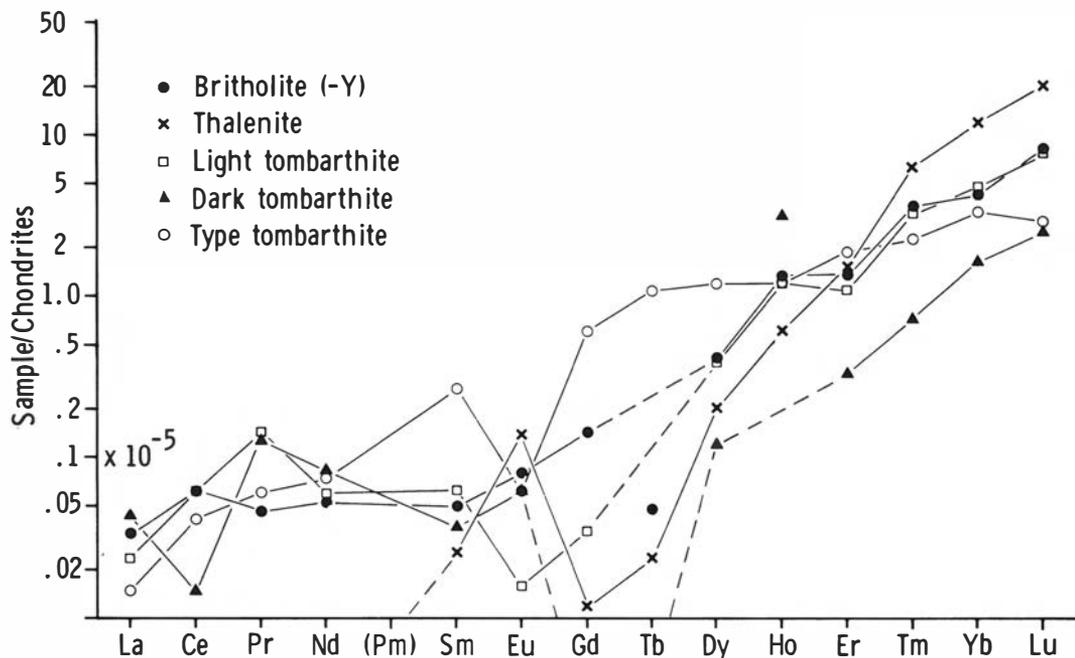
Fig. 2. Chondrite-normalized REE abundances in minerals from Reiarsdal, and in the type tombarthite (Neumann & Nilssen 1968).

& Nilssen 1968). The two analyses presented by Neumann & Nilssen are compared with the microprobe analyses of the present material in Table 2. The two sets are generally similar, apart from the higher MnO and Y_2O_3 contents, and the slightly lower ΣREE, of our material, and the P_2O_5 content (none was detected in the type material).

The structural formulae are in good agreement with the proposed idealized formula RE_4 $(Si+4H)_4O_{12-n}OH_{4+2n}$ (Table 3). Both probe analyses show higher Si, and naturally a greater substitution of $P = Si$. The substitution of H for Si is on the average lower than in the type material, as is the $OH = O$ substitution, but both are still important. All of these differences are easily explainable in terms of the formation of the Reiarsdal material by replacement of britholite.

The REE data show that the lighter variety, which is always closest to the britholite-tombarthite contact, has essentially the same REE content as the britholite. The small negative Eu anomaly is probably not significant, since Eu in the light tombarthite is very near the detection level (100 ppm). The darker tombarthite is more depleted in the heavy REE,
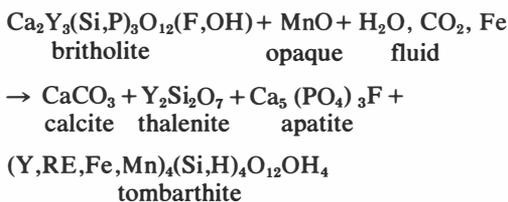
but has LREE similar to the britholite, and does not have a significant Eu anomaly.

The REE data from the type material (Fig. 3) show a strikingly different pattern, with more strongly fractionated LREE, *less* fractionated HREE, and a pronounced negative Eu anomaly. The differences strongly suggest that the type tombarthite formed in equilibrium with feldspar, in a relatively reduced environment. The britholite at Reiarsdal clearly formed together with feldspars, but the environment may have been oxidizing enough to keep Eu in the trivalent state, so that it did not concentrate in the feldspars and thus cause a negative Eu anomaly in the other REE phases. The tombarthite has, in turn, inherited its REE pattern largely from the britholite.

A plot of partition coefficients tombarthite/britholite, like that in Fig. 2, shows an irregular scatter of points near $K_D = 1$ for the lighter phase, and a very indistinct peak near Y for the darker phase. This irregularity, and the heterogeneity of the tombarthite with respect to nearly all elements, suggest that the metasomatic alteration of britholite to tombarthite has involved extensive mobility of chemical components.

Discussion

The petrographic features indicate that a reaction process has been responsible for the formation of tombarthite at Reiarsdal. The primary phases were britholite (-Y) and a Mn-oxide phase. Secondary phases include fluorapatite, thalenite, calcite, and tombarthite. A schematic reaction can be written involving an introduced fluid phase:

$$Ca_2Y_3(Si,P)_3O_{12}(F,OH) + MnO + H_2O, CO_2, Fe$$
britholite   opaque   fluid

$$\rightarrow CaCO_3 + Y_2Si_2O_7 + Ca_5 (PO_4)_3F +$$
calcite   thalenite   apatite

$$(Y,RE,Fe,Mn)_4(Si,H)_4O_{12}OH_4$$
tombarthite

The Ca, P, and F of the britholite have gone into apatite (and calcite), while the Y and REE have entered thalenite and tombarthite. The Th, U from the britholite are now concentrated in the tombarthite (especially the lighter phase), and Mn has concentrated in the darker phase of the tombarthite. The Fe content of the tombarthite must be introduced from outside the britholite 'system'. The HREE from the britholite are slightly concentrated in the thalenite, while the LREE are enriched in the tombarthite. On the whole there do not seem to be any severe qualitative mass-balance problems with the proposed reaction mechanism.

The fact that both thalenite and apatite occur as fracture related inclusions without associated tombarthite, as well as enclosed in tombarthite veins, suggests that the reaction may actually have proceeded in two stages:

(1) britholite + fluids → thalenite + apatite ± calcite
(2) britholite + MnO_2 + fluids → tombarthite ± calcite

The first step would locally deplete the britholite in HREE, and enrich it in Th + U; this may partly explain the heterogeneity of the later tombarthite.

This alteration process probably occurred at a late, low-T stage in the formation of the pegma-

tite. The type tombarthite is intergrown with thalenite, and one may ask if both phases formed by alteration of a pre-existing britholite. The coarseness of the intergrowth, and the differences in chemistry illustrated here, suggest that this is not the case. It is more likely that the two minerals at Høgetveit formed instead of britholite, as a result of environmental factors that remain to be defined. We may, however, expect to find tombarthite as a reaction product in other britholite-bearing pegmatites.

References

Åmli, R. & Griffin, W. L. 1975: Microprobe analysis of REE minerals using empirical correction factors. *Am. Mineral. 60*, 599–606.

Ito, J. 1968: Silicate apatites and oxyapatites. *Am. Mineral. 53*, 890–907.

Jensen, B. B. 1973: Patterns of trace element partitioning. *Geochim. Cosmochim. Acta 37*, 2227–2242.

Kornes, A. N., Batalieva, N. G., Maksimov, B. A., Ilyuhim, V. & Belov, N. V. 1972: Crystal structure of the talenite Y_3 (Si_3O_{10}) OH. *Sov. Phys. Dokl. 17*, 88–90. Translated from Doklady Akademii Nauk SSSR 202, 1324–1327 (1972).

Kupriyanova, I. I. & Sidorenko, G. A. 1963: Minerals of the britholite group. *Doklady Akad. Nauk SSSR 148*, 109–111 (Engl. transl.).

Nagashima, K. & Kato, A. 1966: Chemical studies of minerals containing rarer elements from the Far East district. LX. Thalenite from Suishoyama, Kawamata-machi, Fukushima Prefecture, Japan. *Bull. Chem. Soc. Japan 39*, 925–928.

Nagashima, K., Nakao, K., Wakita, H. & Kato, A. 1971: Chemical studies of minerals containing rarer elements from the Far East district. LXIV. Abukumalitt from Fusamata, Kawamata-machi, Fukushima Prefecture, Japan. *Bull. Chem. Soc. Japan 44*, 867–869.

Neumann, H. & Nilssen, B. 1968: Tombarthite, a new mineral from Högetveit, Evje, South Norway. *Lithos 1*, 113–123.

Pletneva, N., Elina, N. A., Denisov, A. P. & Gavrilov, A. P. 1962: An accessory RE silicate apatite from pegmatites. *In* "Materialy po mineralogii Kol'skogo polustrova". Collection 2, Apatity, 123–132.

Shannon, R. D. & Prewitt, C. T. 1969: Effective ionic radii in oxides and fluorides. *Acta Cryst. B25*, 925–946.

Warshaw, I. & Roy, R. 1964: Crystal chemistry of rare earth sesquioxides, aluminates and silicates. *Progess in Science and Technology of the Rare Earths 1*, 215–221.